AIMS Materials Science, 7(3): 338–353.
DOI: 10.3934/matersci.2020.3.338
Received: 16 April 2020
Accepted: 10 June 2020
Published: 19 June 2020

http://www.aimspress.com/journal/Materials

Research article

Use of spent oil shale to remove methyl red dye from aqueous solutions

Noha Ahmed Mahmoud, Ehssan Nassef* and Mohamed Husain

Department of Chemical Engineering, Faculty of Engineering, Alexandria University, Egypt

* **Correspondence:** Email: ehssan.nassef@pua.edu.eg; Tel: +01111509333.

Abstract: In this study, the efficiency of spent oil shale was assessed to remove the methyl red (MR) from aqueous solution under various chemical and physical parameters. The adsorption kinetics was assessed using the pseudo-first-order and pseudo-second-order models. The results indicated that increase in the level of adsorbent led to an increase in amount of dye removed from the solution. Most of the dye was adsorbed within 90 min. MR adsorption followed pseudo-first-order model. Material extracted oil shale was characterized by several methods such as electronic scanning microscopy (ESM), energy-dispersive X-ray spectroscopy (EDX), and Fourier-transform infrared spectroscopy (FTIR). The treated oil shale showed high adsorption potential against MR in polluted wastewater.

Keywords: spent oil shale; methyl red; wastewater treatment; adsorption

1. Introduction

Recent industrial development has increased the level of wastewater that contains synthetic dyes. Such water leads to pollution of rivers that is harmful for humans. Most of these dyes are azo reactive dyes that contain several azo groups (–N=N–), which impart them bright colors [1,2]. Azo dyes are found in the effluents released by food processing, paper, leather, cosmetics, dye manufacturing, and textile industries [3]. Azo dyes and their breakdown products cause adverse health effects of living organisms [4]. Separation of these dyes from wastewater is not easy owing to their high resistance to treatments with heat, oxidizing agents, and light [1,5]. Integration of several physical, biological, and chemical techniques, such as ultra-filtration, photo-oxidation, coagulation, and electrochemical adsorption, is needed to remove high levels of dyes form wastewater and [6]. In general, the process of adsorption is for the elimination of organic substances, owing to its great efficiency for a broad range of substances [7,8]. In this regard, spent oil shale (or blaes) has attracted a lot of attention owing to its abundance and potential. It can either be used as a capping layer or a general fill. In addition, owing to

its high quality, it could also be used as a sub-base or a selected granular fill. Furthermore, the oil shale can be used, extracted by toluene, as a cheap adsorbent for removal of azo dye from polluted water.

Disposal of spent oil shale is costly and causes environmental issues [9]. Thus, more studies are required to determine viable techniques for safe disposal as well as reuse of spent oil shale as adsorbent. Its viability as an adsorbent is largely attributed to its low cost and high abundance. Oil shale is a sedimentary rock which is a mix of minerals and contains combustible organic matter, including bitumen and kerosene, which essentially makes it a fossil fuel resource. The byproducts of oil shale processing, such as oil shale ash and spent oil shale, could be used as highly efficient adsorbents that can be used to remove methyl red from wastewater [10]. Previous studies have shown that adsorption of reaction dyes using oil shale ash follow the Langmuir isotherms with adsorption capacities of 140 mg/g, 180 mg/g, and 100 mg/g for Drim blue, Drim yellow, and Drim red, respectively [11]. Solution temperature and adsorbent mass ratio affect the level of dye removed from the solution.

Based on their solubility, the dyes can be classified into insoluble dyes, such as sulfur, disperse, acid, and vat dyes, and soluble dyes, such as mordant, direct, metal complex, reactive, acidic, and basic dyes. Acid dye refers to the type of dye that is used at lower pH or in the presence of an acidic solution [12]. Acid dyes are generally used in textile industries for protein fibers, such as animal hair fibers (including alpaca, mohair, and wool). They can also be used to dye silk. Acid dyes interact with the fibers via van der Waals forces, ionic bonds, and hydrogen bonds. Dyes consist of large aromatic molecules containing several linked rings. Acid dyes also contain an amino or sulfonyl group that makes them water-soluble.

One of the most common dyes used in laboratories and for commercial purposes is methyl red (MR). However, it might sensitize skin and eyes or, if swallowed or inhaled, could cause digestive or pharyngeal tract irritation [13,14]. Under aerobic conditions, MR often transforms into N-N'-dimethyl-p-phenylene diamine and 2-aminobenzoic acid [15,16]. Recently there have been several studies that aimed at development of low-cost techniques of removing MR from waste water [17]. In this study, the adsorption efficiency of shale oil waste was evaluated to eliminate MR from effluents.

2. Materials and methods

2.1. Adsorbents

In this study, natural oil shale Egyptian oil shale was used that was obtained from the Al-Quseir region (provided by the EMRA: Egyptian mineral resources authority). Then, the oil shale was crushed and sieved to separate the particles with sizes within the range of 45 and 600 μm.

2.2. Solvent extraction of oil shale

A 50 g of finely ground oil shale sample (0.8–1 mm) was mixed with 100 g of toluene solvent in the three-neck round flask at a liquid:solid mass ratio of 2:1 by wt. The sample was then stirred for 4 h. the solvent was at its boiling point. After the extraction steps were completed, the extraction medium was transferred from the three-neck round flask into a Buckhner funnel and filtered under vacuum through filter paper. The extract collected in the Buckhner flask was then put in a rotary vacuum evaporator until complete evaporation of the solvent was noticed. Figure 1 shows a schematic illustration of the mechanical agitation method of oil extraction derived from oil shale by the organic

solvent. The setup mainly consists of four parts: mechanical stirrer, heater, three-neck flask, and condenser [18,19].

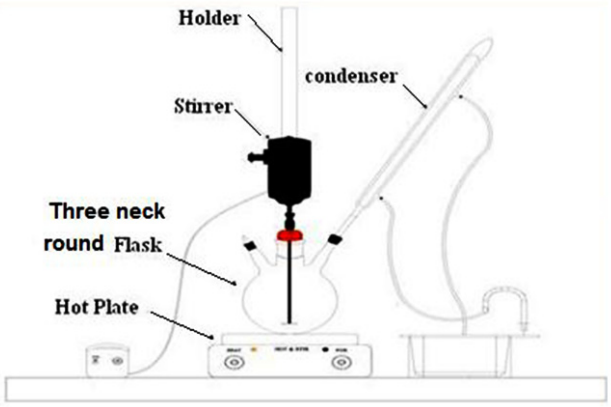

Figure 1. Solvent extraction method for oil recovery.

2.3. Methyl red

MR, 2-[4-(dimethylamino) phenylazo] benzoic acid, a dark red crystalline powder, was used without further purification [20], Figure 2 shows he molecular structure of MR. Its color varies with solution pH. For example, its color is yellow at pH > 6.2, red at pH < 4.4, and orange at pH between 4.4 and 6.2 [21].

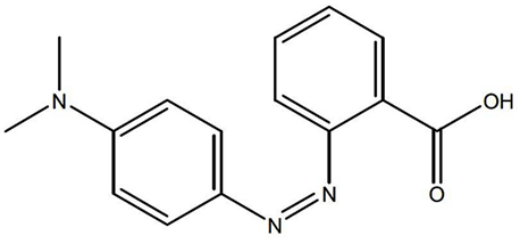

Figure 2. Methyl red structure.

2.4. Methyl red solution preparation

MR stock solution was prepared by dissolving 1 g MR in 1 L of 50% (volume perecnt) ethanol. The stock solution was filtered, covered with aluminium foil, and stored in dark. Working solutions of MR were prepared from the stock solution for further experiments.

3. Procedure

The adsorption experiments were performed using 50 mL dye solutions with varying pH and concentrations. The desired pH of the dye solution was obtained using 0.1 M HCl or 0.1 M NaOH.

Next, 0.6 g of adsorbent was added to each flask, The flasks were then shaken for desired time period and the solutions were centrifuged and filtered to separate the adsorbent from the dye solution.

A UV/Visible spectrophotometer was used to measure the MR level in the solution at 430 nm wavelength [22]. At equilibrium, the adsorbed MR level was evaluated by Eq 1:

$$q_e = \frac{(C_I - C_e)}{W} V \tag{1}$$

whereas, the amount of MR adsorbed at any time was determined by Eq 2:

$$q_t = \frac{(C_I - C_t)}{W} V \tag{2}$$

where q_t and q_e (mg/g) is the level of dye at time (t) and at equilibrium, respectively, C_e and C_I (mg/L) is the equilibrium and initial liquid-phase dye concentration, respectively, W (g) is the adsorbent weight, and V (L) is the initial solution volume.

The level of MR removed via chemically activated oil shale at varying adsorbent weights and duration of treatment and initial concentration was determined by Eq 3:

$$\%R = \frac{C_I - C_F}{C_I} \tag{3}$$

where R is percent removed of the methyl red, C_F and C_I (mg/L) is the final and initial liquid-phase concentration of dye, respectively.

4. Results and discussion

4.1. Spectroscopic study

4.1.1. FTIR analysis

FTIR technique was used to identify the functional groups found in spent oil shale. Figure 3 shows the IR spectra for different functional groups.

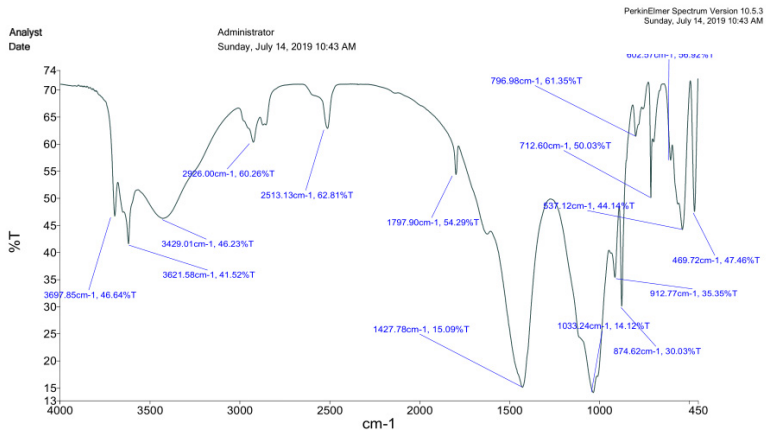

Figure 3. Infrared spectra of spent oil shale.

A wide band in the IR spectra with two maxima at 3697.85 and 3429.01 cm^{-1} was observed. This band could represent stretching mode of the O–H bond found in adsorbed water and hydroxyl groups. Furthermore, such broad peak in the range of 3200–3650 cm^{-1} could represent hydrogen-bonded OH group of phenols and alcohols [23,24]. The peaks at 712.6, 796.98, and 874.62 cm^{-1} could represent out-of-plane C–H bond bending in benzene derivative. The peaks at 1797.9 cm^{-1} could also represent the stretching vibrations of C=O bond with aromatic carbon [25,26]. The peak near 602.57 cm^{-1} could represent C–Br stretching halo compound and peak at 537.12 cm^{-1} is due to C–I stretching halo compound.

Table 1. Infrared spectra of oil shale spent.

Frequency (cm^{-1})	Assignment
3697.85	O–H stretching
3621.58	O–H stretching
3429.01	N–H aliphatic primary amine
2926	C–H alkane
2513.13	C≡N nitrile
1797.9	C=O conjugated acid halide
1427.78	O–H bending
1033.24	None
912.77	None
874.62	C–H bending 1,2,3 trisubstituted
796.98	C–H bending
712.6	benzene derivative
602.57	C–Br stretching halo compound
537.12	C–I stretching halo compound

4.1.2. Energy dispersive analysis of X-rays (EDX)

EDX is used to analyze the elemental composition of individual grains or particles of an SEM sample. In this method, an electron beam interacts with the sample that generates X-rays that are displayed as a spectrum. This spectrum represents the particle's elemental composition [27]. As shown in Figure 4, the distribution of elements can also be mapped using "Dot maps". The elemental analysis shows the presence of carbon (10.24%), oxygen (65.1%), aluminum (1.86%), silicon (9.52%), calcium (8.685%), sulfur (1.76%), and nitrogen (0.57%).

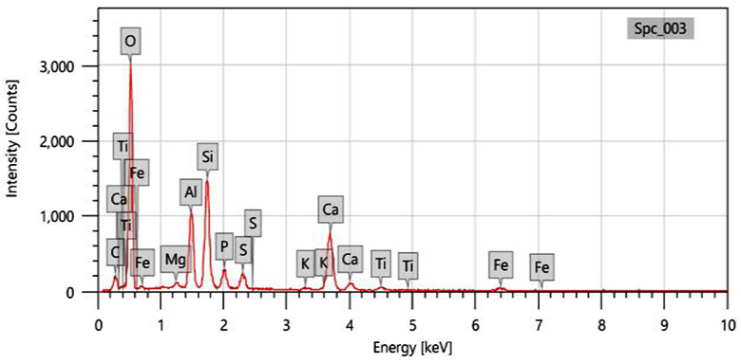

Figure 4. EDX analysis of treated oil shale.

4.1.3. Scanning electron microscope (SEM)

In SEM, the target sample is bombarded with an electron beam for its excitation. The interaction between sample and electron beam generates several signals that could help in elucidating the morphology of sample surface (Figure 5).

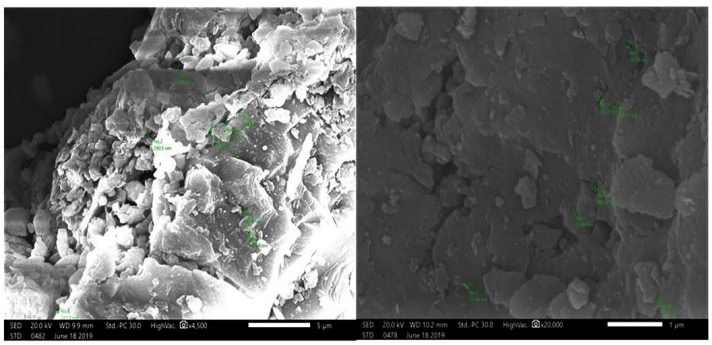

Figure 5. SEM images of treated oil shale.

SEM helps in determination of the characteristics of the microstructure. The secondary electrons produced by the sample's atoms can also be detected by SEM. SEM facilitates topographic imaging of the surface of sample. SEM was used to determine the pore size distribution in the inactivated oil hale sample, since it significantly affects the efficiency of the oil shale to remove MR from the effluents [28]. It was found that the oil shale sample was mainly composed of clay, quartz, and calcite.

4.1.4. Effect of initial dye concentration

A 0.6 g of adsorbent was added in MR solutions with varying dye concentrations (10–100 ppm). The solution was shaken for 90 min and its pH was kept at 10. Figure 6 shows the variation in adsorbed dye quantity against initial concentration of dye in the solution. It was observed that higher the initial dye concentration, lower is the dye removal percentage. At the start of the adsorption process, the adsorbent's surface contains a high number of vacant sites. As the process of adsorption proceeds, the number of such sites decreases [29]. For low dye concentrations, an ample amount of active sites are available on the surface of adsorbent. However, for high MR concentration, there may not be enough vacant active sites. The results were similar to those obtained by previous studies [30].

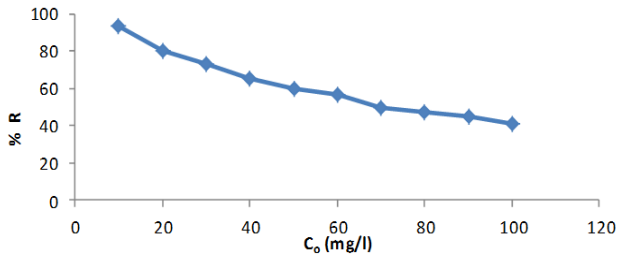

Figure 6. Effect of initial dye concentration on percent dye removal (particle size = 45 µm, 0.6 g of adsorbent, temperature = 30 °C, pH = 10).

4.1.5. Effect of contact time

For a specific initial adsorbate concentration, contact time could help elucidate the adsorption kinetics with a particular adsorbent. Figure 7 shows the effect of contact time on MR adsorption. The percent MR removal increased with increase in contact time for up to 90 min, and then, it reached equilibrium. This result could be attributed to high abundance of active sites on adsorbent's surface at the start of adsorption. As the adsorption proceed, most of these sites are filled, making the filling of remaining sites increasingly difficult owing to the repulsion between the solute molecules on adsorbent surface and those in solution [31].

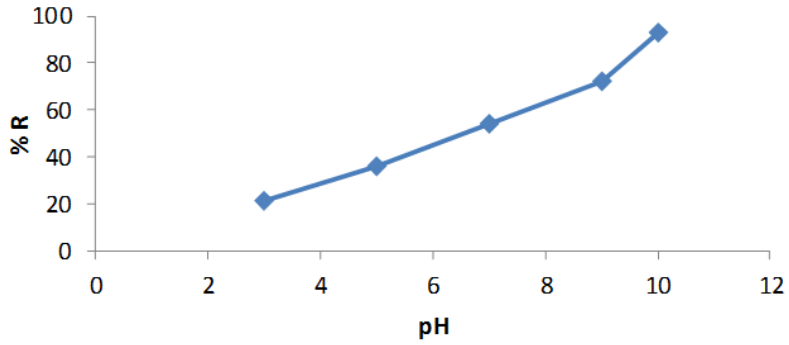

Figure 7. Effect of contact time on percent dye removal at varying initial concentrations of dye (practical size = 45 µm, 0.6 g of adsorbent, temperature = 25 °C, pH = 7).

4.1.6. Effect of adsorbent weight

Different quantities of adsorbent (0.1–0.6 g) were added into 50 mL MR solutions with varying dye concentrations, and agitated the mixture at 120 rpm for 90 min. This was done to determine the adsorbent weight required to achieve optimum adsorption. Figure 8 shows increase in the output with the addition of OSA to up to 0.6 g and reached a maximum value, then it stabilized. This trend could be attributed to rise in number of adsorption sites and sorptive surface area [32].

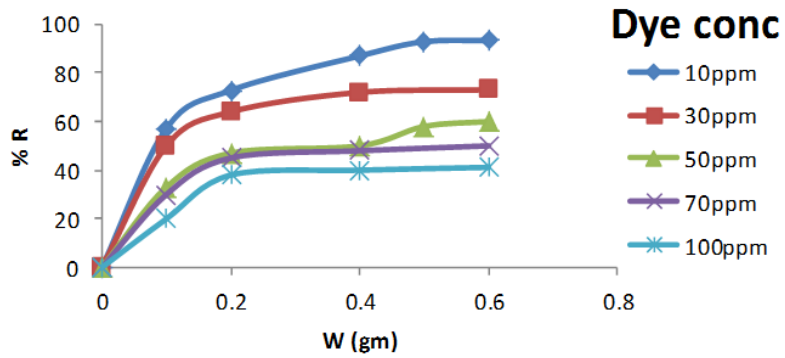

Figure 8. Effect of adsorbent weight on MR adsorption at different initial concentration of dye (practical size = 45 µm, temperature = 30 °C, pH = 10).

4.1.7. Effect of initial pH

Different MR solutions with varying pH (3–10) were prepared to assess the effect of pH on adsorption of MR. At an initial dye concentration of 10 ppm, the effect of pH on MR dye removal is depicted in Figure 9. Higher pH led to higher MR removal percent. The change in solution pH causes alteration in the surface characteristics of adsorbent that affects its adsorption efficiency [33].

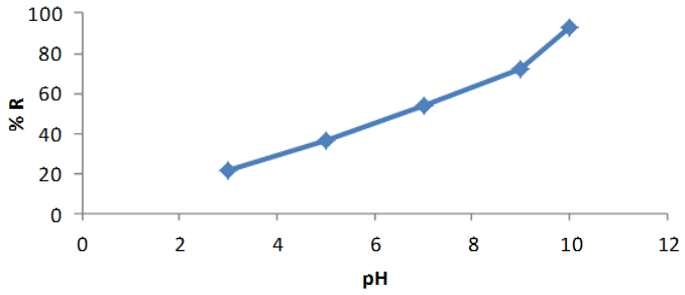

Figure 9. Effect of pH on (MR) adsorption by 0.6 gm. oil shale ash with initial concentration of 10 ppm and particle size 45 µm for 90 min.

4.1.8. Effect of particle size

The effect of oil shale particle sizes on percent dye removal was assessed by preparing 50 mL dye solutions (pH 7) with varying dye concentrations and adding the adsorbent with varying particle sizes (45, 75, 150, 300, and 600 µm) (Figure 10).

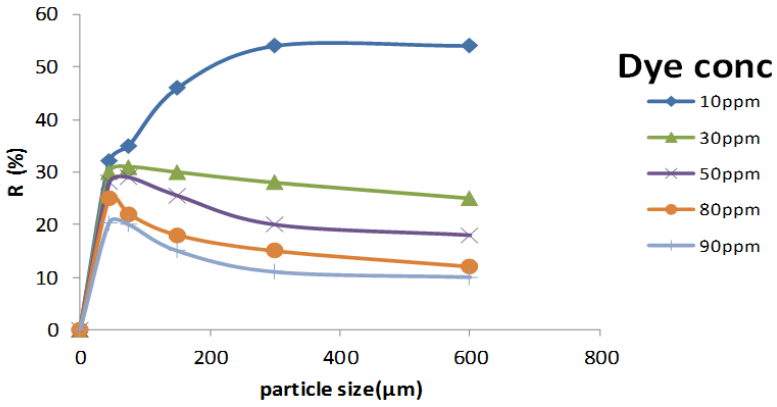

Figure 10. Effect of particle size on percent dye removal at different initial dye concentration (practical size = 45 µm, 0.6 g of adsorbent, temperature = 25 °C, pH = 7).

It was observed maximal dye removal in presence of adsorbent with particle size of 45 µm for all dye concentrations. Reduction in particle size increases the adsorption surface area. Thus, higher level of adsorption due to smaller adsorbent particles could be attributed to a larger surface area and higher pore accessibility [34,35].

4.1.9. Effect of temperature

Next, MR solutions with varying MR concentrations was prepared (10–100 ppm) and 0.6 g adsorbent and carried out adsorption at varying solution temperatures (20 °C, 25 °C, 30 °C). As shown in Figure 11, higher solution temperature led to a higher percent dye removal. This result could be attributed to decrease in solution viscosity with increase in its temperature, which subsequently enhances the diffusion rate of dye to internal pores and external layer of spent oil shale [36].

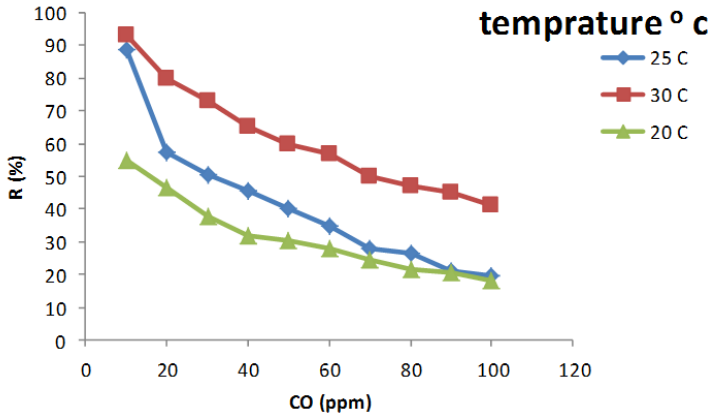

Figure 11. Effect of temperature on percent dye removal at different initial dye concentrations (practical size = 45 μm, 0.6 g of adsorbent, pH = 10).

4.2. Adsorption isotherms

An adsorption isotherm reflects the diffusion pattern of adsorbed molecules across solid and liquid phases during equilibrium state of adsorption.

Fitting of data into various isotherm models is crucial in identifying the optimum model for a particular adsorption process. Such isotherms often help elucidate the interaction between solute and adsorbent and facilitate optimization of adsorption process [37].

In this study, three models were used for the adsorption isotherm study: Langmuir, Freundlich, and Temkin isotherm model. Correlation coefficient, R^2 was calculated to verify if these models are applicable to this study.

4.2.1. Langmuir isotherm model

Langmuir isotherm model assumes that adsorption energies do not vary across the surface and the adsorbate does not emigrate from plane of surface. It works on the hypothesis of no interaction between adsorption energy and adsorbed molecules across the adsorbent's surface. In addition, this model also assumes that decrease in distance leads to rapid decrease in intermolecular forces, and thus, considers spent oil shale powder to be of monolayer type, that is, when an adsorbate molecule attaches to a site on the adsorbent, that site does not participate in any further adsorption [38]. The Eq 4 represents a linear Langmuir isotherm model:

$$\frac{C_e}{q_e} = \frac{1}{q_{max} K_L} + \frac{C_e}{q_{max}} \quad (4)$$

where:
C_e = Adsorbate concentration at equilibrium (mg/L)
q_e = The amount of adsorbate adsorbed per unit mass of adsorbent (mg/g)
K_L and q_{max} = Langmuir constants for adsorption rate and capacity, respectively.

Figure 12 shows that a plot of C_e/q_e vs C_e is a straight line with $1/q_{max}$ as slope. A q_{max} of 3.8 and K_l of 0.14475 from the plot was obtained. The correlation coefficient, R^2, was 0.983.

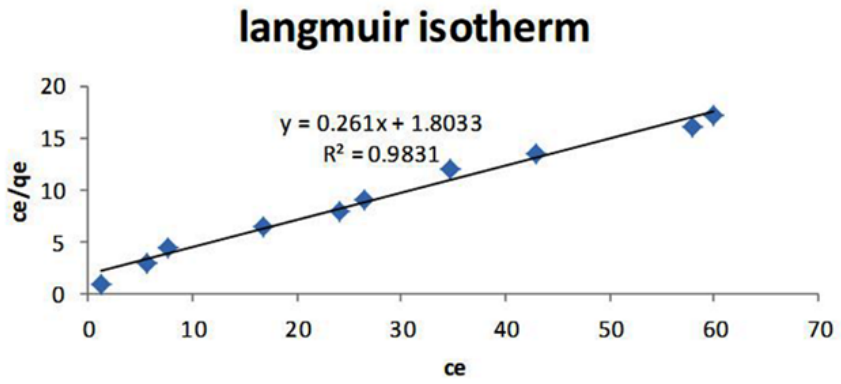

Figure 12. Langmuir isotherm for MR sorption onto spent oil shale.

Langmuir isotherm can essentially be represented in the terms of separation factor (R_L), which is a constant without a dimension.

$$R_L = \frac{1}{1 + K_L C_0} \quad (5)$$

R_L value determines whether the isotherm is irreversible ($R_L = 0$), linear ($R_L = 1$), favorable ($0 < R_L < 1$), or unfavorable ($R_L > 1$). R_L values in the model indicated that the isotherm was favorable at all concentrations analyzed (Eq 5).

4.2.2. The Freundlich isotherm

Freundlich isotherm model represents an empirical equation that can help in assessing a non-ideal sorption process, including heterogeneous adsorption [39,40]. The Freundlich isotherm is described using a non-linear equation that is constructed on the basis of an assumption that increase in proportion of occupied sites leads to a logarithmic decrease in the adsorption enthalpy.

$$q_e = K_F C_e^{\frac{1}{n}} \quad (6)$$

K_F is a constant that is associated with bonding energy. It represents a coefficient of distribution or adsorption. It indicates the amount of adsorbed dye per unit equilibrium concentration. The surface

heterogeneity of adsorbent is represented by 1/n; closer the value of 1/n to zero, higher the heterogeneity of the surface. 1/n < 1 represents Langmuir adsorption, whereas 1/n > 1 represents Freundlich isotherm (cooperative adsorption). Freundlich isotherm model can be represented as Eq 7:

$$\ln q_e = \ln K_F + \frac{1}{n} \ln C_e \tag{7}$$

A plot between ln q_e and ln C_e is also helpful in assessing the applicability of Freundlich adsorption isotherm (Figure 13). Table 2 shows the Freundlich isotherm plot data for the study. For both isotherms, the high values of coefficients of correlation indicated that Langmuir model is comparable to Freundlich model. 1/n < 1 indicated a favorable adsorption of MR by spent oil shale.

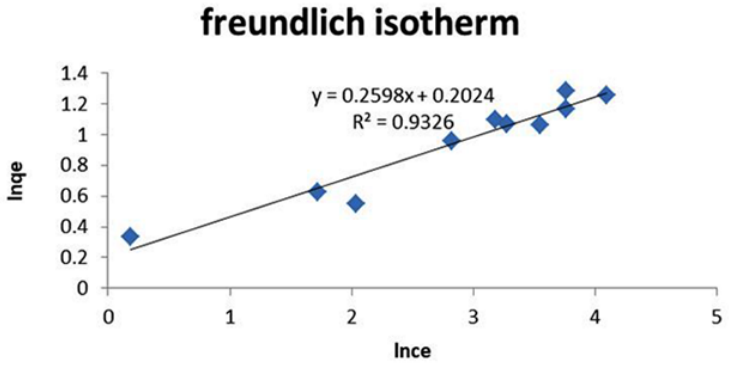

Figure 13. Freundlich isotherm for MR sorption onto spent oil shale.

Table 2. Comparison of isotherm parameters for MR adsorption (concentration of spent oil shale: 0.6 g/50 mL).

	Langmuir	
	Q_m (mg/g)	3.831
	K_L (L/mg)	0.144
	R^2	0.983
Freundlich	1/n	0.259
	K_F (mg/g)	1.224
	R^2	0.932
Tempkin	K_T (L^{-1})	5.091
	B (mg^{-1})	0.599
	B(J/MOL)	4134.799
	R^2	0.893

4.2.3. The Tempkin isotherm

Tempkin isotherm model assumes a linear reduction in the heat of adsorption, contrary to the logarithmic decrease assumed for Freundlich isotherm model. The Tempkin isotherm model can be represented as Eq 8:

$$q_e = \frac{RT}{b} \ln K_T C_e \tag{8}$$

This equation can be simplified as Eq 9:

$$q_e = B \ln K_T + B \ln C_e \tag{9}$$

where (RT/b) = B, R = universal gas constant, and T = absolute temperature (in Kelvin). The constant b indicates heat of adsorption [40,41]. The data was analyzed using the linear Tempkin isotherm equation (Eq 9). The Tempkin isotherm model fit well with the data. Table 2 and Figure 14 show the values of coefficients and linear isotherm constants. R^2 value for Tempkin isotherm model was comparable to R^2 values from Langmuir and Freundlich isotherm models. It indicated that the Tempkin model was applicable for the data.

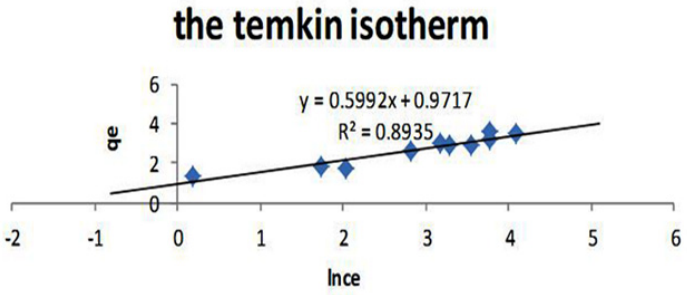

Figure 14. Tempkin isotherm for MR sorption onto spent oil shale.

4.3. Adsorption kinetics

Analysis of adsorption kinetics is crucial to determine the operating conditions that are optimum for a full-scale batch process. It facilitates prediction of the adsorption rate and designing of adsorption processes. The adsorption kinetics of MR was studied using pseudo-first-order and pseudo-second-order models [42].

4.3.1. Lagergren pseudo-first-order

The adsorption kinetics was analyzed using the Lagergren pseudo-first-order model [41], which can be represented as Eq 10:

$$\log(q_e - q_t) = \log q_e - k_1 t \tag{10}$$

where q_t and q_e = the amounts of MR adsorbed (mg g^{-1}) at time (t) (min) and equilibrium, respectively.

Log($q_e - q_t$) vs t plots helped in determining the k_1 values for varying initial MR concentrations (Figure 15). High R^2 values (>0.97) showed that the experimental q_e was comparable to the calculated q_e for each MR concentration (Figure 15 and table 3). It indicated that the model was applicable to the adsorption process.

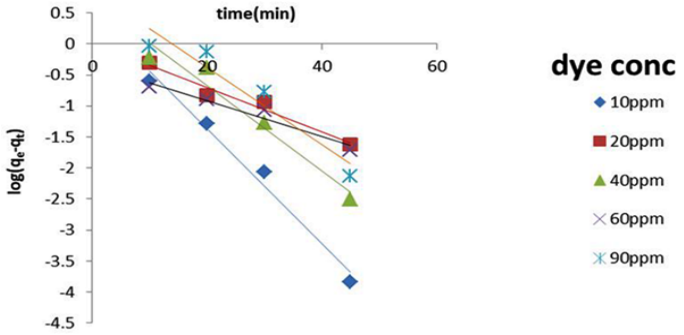

Figure 15. Pseudo-first-order kinetics for MR sorption onto spent oil shale.

Table 3. Summarized data of variables and constants of pseudo-first-order and pseudo-second-order.

Initial concentration (mg/L)	Pseudo-first-order				Pseudo-second-order		
	$q_{e(exp}$	k_1	$q_{e(cal}$	R^2	k_2	$q_{e(cal}$	R^2
10	0.817	−0.092	1.611	0.981	0.048	1.034	0.967
20	0.924	−0.035	1.016	0.963	0.010	1.590	0.874
40	1.114	−0.066	1.758	0.981	0.013	1.739	0.953
60	1.235	−0.021	0.623	0.991	0.055	1.392	0.986
90	1.421	−0.059	1.930	0.972	0.011	2.170	0.9782

4.3.2. Pseudo-second-order

Pseudo-second-order model is based on equilibrium adsorption [40–42] and can be represented as Eq 11:

$$\frac{t}{q_t} = \frac{1}{k_2 q_e^2} + \frac{t}{q_e} \tag{11}$$

where k_2 (g/mg min) represents the rate constant of second-order adsorption process. Linear t/q_t vs t plot revealed low R^2 values, which indicated that the experimental and calculated q_e values differed significantly (Figure 16, Table 3).

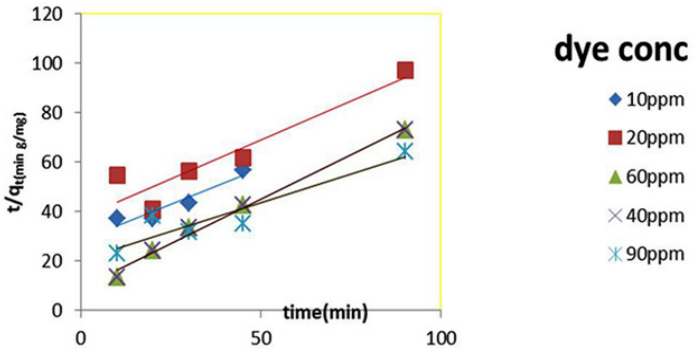

Figure 16. Pseudo-second-order for MR adsorption.

5. Conclusion

Oil shale was treated using solvent extraction and used for MR removal from wastewater. Maximum MR adsorption occurred at pH 10. At initial dye concentration range of 10–100 mg/L, the adsorption process took 90 min to reach equilibrium. The data was analyzed using Freundlich, Tempkin, and Langmuir isotherm models. All the models were applicable for the data as shown by R^2 values. A monolayer L-type isotherm best described the adsorption process. Pseudo-first-order and pseudo-second-order models were used to assess the adsorption kinetics. The results revealed that the adsorption process followed pseudo-first-order kinetics. The results indicated that oil shale, treated by toluene, exhibited high potential as a cheap adsorbent for MR removal from wastewater.

Conflict of interests

The authors decalre that they have no conflcit of interest.

References

1. Crini G (2006) Non-conventional low-cost adsorbents for dye removal: a review. *Bioresource Technol* 97: 1061–1085.
2. Robinson T, McMullan G, Marchant R, et al. (2001) Remediation of dyes in textile effluent: a critical review on current treatment technologies with a proposed alternative. *Bioresource Technol* 77: 247–255.
3. Aksu Z (2005) Application of biosorption for the removal of organic pollutants: a review. *Process Biochem* 40: 997–1026.
4. Han R, Zhang J, Zou W, et al. (2005) Equilibrium biosorption isotherm for lead ion on chaff. *J Hazard Mater* 125: 266–271.
5. Gupta VK, Ali I, Mohan D, et al. (2003) Equilibrium uptake and sorption dynamics for the removal of a basic dye (basic red) using low-cost adsorbents. *J Colloid Interf Sci* 265: 257–264.
6. Ho YS, Chiu WT, Wang CC (2005) Regression analysis for the sorption isotherms of basic dyes on sugarcane dust. *Bioresource Technol* 96: 1285–1291.
7. Kumar KV (2006) Comparative analysis of linear and non-linear method of estimating the sorption isotherm parameters for malachite green onto activated carbon. *J Hazard Mater* 136: 197–202.
8. Ghimire KN, Inoue K, Miyajima T, et al. (2001) Adsorption of some metal ions and mineral acids on chitin. *J Chitin Chitosan Sci* 7:61–68.
9. Al-Hamaiedh H, Maaitah O, Mahadin S (2010) Using oil shale ash in concrete binder. *Electron J Geotech Eng* 15: 601–608.
10. Al-Qodah Z (2000) Adsorption of dyes using shale oil ash. *Water Res* 34: 4295–4303.
11. Santhi T, Manonmani S, Smitha T (2010) Removel of methyl red from aqueous solution by activated carbon preparted from the *Annona squmosa* seed by adsorption. *Chem Eng Res Bull* 14: 11–18
12. Mitchell E, Frisbie S, Sarkar B (2011) Exposure to multiple metals from groundwater—a global crisis: Geology, climate change, health effects, testing, and mitigation. *Metallomics* 3: 874–908.

13. Hayes BB, Azadi S, Sullivan RR, et al. (2004) Contact hypersensitivity to methyl red in female Balb/c mice. *J Allergy Clin Immun* 113: S57.
14. Badr Y, El-Wahed MA, Mahmoud MA (2008) Photocatalytic degradation of methyl red dye by silica nanoparticles. *J Hazard Mater* 154: 245–253.
15. So KO, Wong PK, Chan KY (1990) Decolorization and biodegradation of methyl red by Acetobacter liquefaciens. *Toxicity Assess* 5: 221–235.
16. Jadhav SU, Kalme SD, Govindwar SP (2008) Biodegradation of methyl red by Galactomyces geotrichum MTCC 1360. *Int Biodeter Biodegr* 62: 135–142.
17. Aksu Z, Dönmez G (2003) A comparative study on the biosorption characteristics of some yeasts for Remazol Blue reactive dye. *Chemosphere* 50: 1075–1083.
18. Soliman A (2015) Extraction of oil from Egyptian oil shale. *International Conference and Expo on Oil and Gas*, Dubai, UAE.
19. Nassef E, Soliman A, Al-Alla RA, et al. (2015) Experimental study on solvent extraction of Quseir oil shale in Egypt. *JSEMAT* 5: 147–152.
20. Adowei P, Horsfall Jr M, Spiff AI (2012) Adsorption of methyl red from aqueous solution by activated carbon produced from cassava (Manihot esculenta Cranz) peel waste. *Innov Sci Eng* 2: 24–33.
21. Saiful Azhar S, Abdul Ghaniey Liew A, Suhardy D, et al. (2005) Dye removal from aqueos solution by using adsorption on treated sugarcane bagasse. *Am J Eng Appl Sci* 2: 1499–1503.
22. Rana SV (2014) Perspectives in endocrine toxicity of heavy metals—a review. *Biol Trace Elem Res* 160: 1–4.
23. Sheng PX, Ting YP, Chen JP, et al. (2004) Sorption of lead, copper, cadmium, zinc, and nickel by marine algal biomass: characterization of biosorptive capacity and investigation of mechanisms. *J Colloid Interf Sci* 275: 131–141.
24. Gorzin F, Ghoreyshi AA (2013) Synthesis of a new low-cost activated carbon from activated sludge for the removal of Cr (VI) from aqueous solution: Equilibrium, kinetics, thermodynamics and desorption studies. *Korean J Chem Eng* 30: 1594–1602.
25. Levankumar L, Muthukumaran V, Gobinath MB (2009) Batch adsorption and kinetics of chromium (VI) removal from aqueous solutions by Ocimum americanum L. seed pods. *J Hazard Mater* 161: 709–713.
26. Bansal M, Singh D, Garg VK (2009) A comparative study for the removal of hexavalent chromium from aqueous solution by agriculture wastes' carbons. *J Hazard Mater* 171: 83–92.
27. Giri AK, Patel R, Mandal S (2012) Removal of Cr (VI) from aqueous solution by Eichhornia crassipes root biomass-derived activated carbon. *Chem Eng J* 185: 71–81.
28. Goldstein JI, Newbury DE, Michael JR, et al. (2003) *Scanning Electron Microscopy and X-ray Micronalysis*, 3rd Eds., New York: Plenum Press.
29. El Nemr A, Abdelwahab O, El-Sikaily A, et al. (2009) Removal of direct blue-86 from aqueous solution by new activated carbon developed from orange peel. *J Hazard Mater* 161: 102–110.
30. Hameed BH, Ahmad AL, Latiff KN (2007) Adsorption of basic dye (methylene blue) onto activated carbon prepared from rattan sawdust. *Dyes Pigments* 75: 143–149.
31. Gulipalli CS, Prasad B, Wasewar KL (2011) Batch study, equilibrium and kinetics of adsorption of selenium using rice husk ash (RHA). *J Eng Sci Technol* 6: 586–605.

32. Mittal A, Gupta VK, Malviya A, et al. (2008) Process development for the batch and bulk removal and recovery of a hazardous, water-soluble azo dye (Metanil Yellow) by adsorption over waste materials (Bottom Ash and De-Oiled Soya). *J Hazard Mater* 151: 821–832.
33. Santhi T, Manonmani S, Smitha T (2010) Removal of methyl red from aqueous solution by activated carbon prepared from the *Annona squmosa* seed by adsorption. *Chem Eng Res Bull* 14: 11–18.
34. Ofomaja AE (2008) Kinetic study and sorption mechanism of methylene blue and methyl violet onto mansonia (Mansonia altissima) wood sawdust. *Chem Eng J* 143: 85–95.
35. Krishna RH, Swamy AV (2012) Investigation on the effect of particle size and adsorption kinetics to removal of hexavalent chromium from the aqueous solutions using low cost sorbent. *Eur Chem* 1: 258–262.
36. Gürses A, Hassani A, Kıranşan M, et al. (2014) Removal of methylene blue from aqueous solution using by untreated lignite as potential low-cost adsorbent: kinetic, thermodynamic and equilibrium approach. *J Water Process Eng* 2: 10–21.
37. Nasuha N, Zurainan HZ, Maarof HI, et al. (2011) Effect of cationic and anionic dye adsorption from aqueous solution by using chemically modified papaya seed. *International Conference on Environment Science and Engineering* 8: 50–54.
38. Baek MH, Ijagbemi CO, Se-Jin O, et al. (2010) Removal of Malachite Green from aqueous solution using degreased coffee bean. *J Hazard Mater* 176: 820–828.
39. Aharoni C, Sparks DL (1991) Kinetics of soil chemical reactions—a theoretical treatment, In: Sparks DL, Suarez DL, *Rates of soil Chemical Processes*, Soil Science Society of America,27: 1–18.
40. Akkaya G, Özer A (2005) Biosorption of Acid Red 274 (AR 274) on Dicranella varia: Determination of equilibrium and kinetic model parameters. *Process Biochem* 40: 3559–3568.
41. Lagergren SK (1898) About the theory of so-called adsorption of soluble substances. Sven. Vetenskapsakad. *Handingarl* 24: 1–39.
42. Ho YS, McKay G, Wase DA (2000) Study of the sorption of divalent metal ions on to peat. *Adsorpt Sci Technol* 18: 639–650.